Numerical Modeling of Changes In Groundwater Storage And Nitrate Load in The Unconfined Aquifer Near a River Receiving Reclaimed Water

Ruixue Jiang (ruixue_jiang@163.com)
Institute of Geographic Sciences and Natural Resources Research Chinese Academy of Sciences
https://orcid.org/0000-0003-3469-1842

Dongmei Han
Institute of Geographic Sciences and Natural Resources Research Chinese Academy of Sciences

Xianfang Song
Institute of Geographic Sciences and Natural Resources Research Chinese Academy of Sciences

Fandong Zheng
Beijing Water Science and Technology Institute

Research Article

Keywords: Reclaimed water, Unconfined aquifer, Groundwater table, Groundwater storage, Nitrate loads, Numerical model

Posted Date: November 3rd, 2021

DOI: https://doi.org/10.21203/rs.3.rs-1033197/v1

Version of Record: A version of this preprint was published at Environmental Science and Pollution Research on January 21st, 2022. See the published version at https://doi.org/10.1007/s11356-022-18597-1.

Abstract

Reclaimed water (RW) has been widely used as an alternative water resource to recharge rivers in mega-city Beijing. At the same time, the RW also recharges the ambient aquifers through riverbank filtration, and modifies the subsurface hydrodynamic system and hydrochemical characteristics. To assess the impact of RW recharge on the unconfined groundwater system, we conducted a 3D groundwater flow and solute transport model based on 10 years of sequenced groundwater monitoring data to analyze the changes of the groundwater table, Cl^- loads, and NO_3-N loads in the shallow aquifer after RW recharge to the river channel. The results show that the groundwater table around the river channel elevated by about 3~4 m quickly after RW recharge from Dec. 2007 to Dec. 2009, and then remained stable due to the continuous RW infiltration. However, the unconfined groundwater storage still declined overall from 2007 to 2014 due to groundwater exploitation. The storage began to recover after groundwater extraction reduction, rising from 3.76×10^8 m^3 at the end of 2014 to 3.85×10^8 m^3 at the end of 2017. Cl^- concentrations varied from 5~75 mg/L before RW recharge to 50~130 mg/L in two years (2007–2009), and then remained stable. The zones of the unconfined groundwater quality-affected by RW infiltration increased from 11.7 km^2 in 2008 to 26.7 km^2 in 2017. Cl^- loads of the unconfined groundwater increased from 1.66×10^4 t in 2008 to 3.8×10^3 t in 2017, while NO_3-N loads decreased from 29.8 t in 2008 to 11.9 t in 2017 annually in the zones. We determined the maximum area of the unconfined groundwater quality affected by RW, and groundwater outside this area not affected by RW recharge keeps its original state. The RW recharge to the river channel in the study area is beneficial to increase the groundwater table and unconfined groundwater storage with lesser environmental impacts.

1 Introduction

The increasing demands for water resources driven by a combination of population growth, socio-economic development, rapid urbanization, and climate change have been led to water scarcity and quality deterioration (USEPA and USAID, 2012; WWAP, 2019). Facing the ongoing enormous stresses and challenges, reclaimed water (RW) treated from wastewater has been increasingly used as an alternative water resource for different purposes (Asano, 2007; Ahuja, 2015; Deng et al., 2019). RW could be utilized for agricultural irrigation, landscape irrigation, industrial reuse, municipal water, and groundwater recharge (Angelakis and Gikas, 2014; De Gisi et al., 2017; Deng et al., 2019). RW helps increase the reliability of sustainable water supply in many water-scarce areas of the world (Angelakis et al., 2018; Hess and Collins, 2019; Kog, 2020; Tortajada and van Rensburg, 2020; Zhu and Dou, 2018).

In China, RW utilization was 2.17×10^9 in 2009, accounting for 0.36% of the total water supply amount (Zhu and Dou, 2018). Then it was up to 8.74×10^9 m^3 in 2019, accounting for 1.5% of the total water supply amount (MWR, 2021). Beijing, as a mega-city with serious water shortages, being characterized by drying some rivers with a degraded ecosystem, is the biggest RW user in China (Zhang et al., 2014; MWR, 2021). The amount of Beijing's RW utilization was 6×10^8 in 2008, accounting for 17% of the total water supply amount, while it was up to 2×10^9 m^3 in 2020, accounting for approximately 30% of the total water

supply amount (Beijing Water Authority, 2020). Over 90% of the RW was primarily used for purposes of recreation and ecological conservation (e.g. water supply for recharging rivers or lakes) (Beijing Water Authority, 2019). But compared with other natural water types, RW usually contains higher levels of salts, nitrogen, phosphorus, heavy metals, organic, and biological contaminants, which are controlled by the water treatment technologies (Deng et al., 2019; Valhondo et al., 2020). As a result, groundwater may have potential health risks and environmental impacts as RW seeps into the aquifer by river leakage (Asano and Cotruvo, 2004; Bekele et al., 2018).

It has been demonstrated that some contaminants' concentrations may decrease during the RW infiltration process (e.g., filtration, adsorption, redox reaction, and degradation), such as nutrients (Singer and Brown, 2018), total organic carbon (Bekele et al., 2011), heavy metals (Zhang et al., 2020), trace organic compounds (Li et al., 2015; Ding et al., 2020), and pathogen (Page et al., 2010). RW recharge also changes the interaction of surface water-groundwater and related hydraulic features (Guo et al., 2019; Yuan et al., 2020). Hydrochemical components of groundwater could be modified by the RW mixing with native groundwater along the flow path (Yu et al., 2016; Gilabert-Alarcón et al., 2018; Daesslé et al., 2020). Additionally, the dissolved ions, including arsenic (Fakhreddine et al., 2021) and metals (Davranche and Bollinger, 2000; Patterson et al., 2010) in sediments, can be released into groundwater during the geochemical processes. It brings risks and challenges for water resources management.

The Shunyi reaches of the Chaobai River in Beijing have been dried since 2000, which RW has utilized for recharging river since December 2007 to improve the aquatic ecological conservation of the dry river. Many studies have been carried out on characterizing variations in physical and chemical parameters of groundwater after RW recharge in the study area, with the most significant changes in the unconfined aquifer. The groundwater table increased by ~3 m after RW supply to the Chaobai River from 2007 to 2018 (He et al., 2021). Column experimental results indicated that cation exchange took place between K^+ in the RW and Ca^{2+} in the riverbed medium during RW infiltration (Liu et al., 2018). The hydrochemical type of the unconfined groundwater has been obviously modified from HCO_3-Ca·Mg in 2007 to HCO_3·Cl-Na·Ca·Mg in 2018, the latter is similar to the RW type (HCO_3·Cl-Na·Ca and HCO_3·SO_4·Cl-Na·Ca) (Li et al., 2019; Jiang et al., 2020; He et al., 2021). It has been observed that salinities of the unconfined groundwater increased, and the total hardness decreased (Liu et al., 2018). Nitrogen (including NO_3-N, NO_2-N, and NH_4-N) (Liu et al., 2018; Li et al., 2019) and some endocrine-disrupting chemicals (Li et al., 2013a; Ma et al., 2015; Wang et al., 2019) was observed to be removed during the infiltration process with different removal rates in the column experiments and field monitoring. Nitrogen, especially nitrate, is the typical contaminant in the RW, river, and unconfined groundwater in this area (Yang et al., 2016; Li et al., 2019).

However, few studies have focused on quantifying the effects of RW recharge on the groundwater system. Numerical modeling can be applied to predict groundwater flow and solute transport and evaluate the impacts of human activities (Machiwal et al., 2018; Sege et al., 2018).

The objectives of this study are to (i) conduct a 3D groundwater flow and solute (Cl^-) transport model, (ii) calculate the changes of unconfined groundwater storage, Cl^- loads, and NO_3-N loads, and (iii) identify the area of groundwater quality affected by the RW recharge and illustrate the environmental impacts in the study area. It can improve understanding of the effects of RW recharge to a river channel on the groundwater system and provide a scientific reference for the safe use of RW and water resources management in other similar regions globally.

2 Material And Methods

2.1 Study area

The study area is located in the northeast of Beijing, between longitudes 116°36' to 116°46' E and latitudes 40°02' to 40°12' N (Fig. 1a). Elevation ranges between 22 m and 54 m.a.s.l (Aji et al., 2008). The area is in the northern temperate region, with a typical continental monsoon climate. The annual average temperature is ~11.5°C. The mean annual precipitation is about 610 mm, chiefly from June to September. The average annual evaporation based on pan evaporation experiments is about 1108 mm.

The Jian River is an artificial channel with a natural river bottom and sloping brick sides. It is about 4 km long, 50~90 m wide, and holds approximately $5.1 \cdot 10^5$ m^3 of water. The Chaobai River in the study area is a natural channel. It is about 15 km long, 200~400 m wide, and holds approximately $8.91 \cdot 10^6$ m^3 of water.

The Chaobai River channel was dry before 2007. Beijing Municipal Water Diversion Project was implemented for restoring the dry river channel by Beijing Water Authority since 2007. The Wenyu River water was pumped and treated by a membrane bioreactor (MBR) to produce RW. Then the RW was transferred into the Jian River and finally flowed into the Chaobai River (Fig. 1a). The transferred volume of RW is $2.9 \cdot 10^7$ m^3 in 2017, and the cumulative transferred volume is $2.3 \cdot 10^8$ m^3 from 2007 to 2017. Dams are set up to control the river water level and separate reaches of the river. RW has replenished the Jian River and Shunyi reach of the Chaobai River since October 2007. The section from the earth dam to the Henan rubber dam (Fig. 1a) is a perennial water-receiving river channel. The section between the Xiangyang sluice and the earth dam is replenished only in May and October as an intermittent water-receiving river channel. Moreover, the section from the Henan rubber dam to the Suzhuang rubber dam has been perennially replenished since 2012.

2.2 Hydrogeology conditions

The study area locates at the edge of the alluvial fan of the Chaobai River. Stratigraphic distribution can be seen from the hydrogeological profile (Fig. 1b), which is characterized by some interbedded layers. From north to south, sediment grains gradually change from coarse to fine. There are three aquifers of different depths, and each aquifer expresses as the mean depth of the bottom is 30 m, 50 m, and 80 m,

which are mainly composed of gravel and coarse sand (Li et al., 2013b) and separated by clay-rich aquitards. The top 30 m-depth aquifer is unconfined, and 50 m- depth and 80 m-depth aquifers are confined. The main groundwater pumping layer is the aquifer below 80 m-depth.

The groundwater is mainly recharged by rainfall, river leakage, lateral inflow, and irrigation seepage through the upper aquifer. Groundwater exploitation is the main way of discharge. The average depth of groundwater table in the Xiangyang sluice (G01, G02, and G03) was 29.7 m in 2017, and the average depth for other monitoring wells in Fig. 1a was 4.4 m in 2017. The groundwater generally flows from southwest to northeast, which is opposite to the terrain due to the excessive groundwater exploitation (Zheng et al., 2015).

2.3 Data sources

Details on input data are summarized in Table 1. All the data were processed into a monthly dataset from December 2007 to December 2017, analyzed for setting up a conceptual model, and finally converted into a numerical model for groundwater flow and solute transport simulation.

Table 1
Groundwater flow and transport model input data

Input data	Source	Data preparation and main values
Ground elevation	the Advanced Spaceborne Thermal Emission and Reflection Radiometer Global Digital Elevation Model (resolution of 1 arc-second)	22~54 m
Layers' thickness	Data from 14 Boreholes, provided by Beijing Water Science and Technology Institute (BWSTI)	The thickness of the seven layers is 10~55 m, 1~32 m, 1~29 m, 1~26m, 1~15 m, 1~19 m, and 104~150 m from top to bottom.
RW infiltration	Monthly and annual data of RW transfer volume are provided by BWSTI.	Average RW transfer volume: 2.3×10^7 m^3/a (2008-2017). The infiltration amount of RW was calculated by water balance and then adjusted during the calibration process.
Groundwater withdrawal	(Zheng, 2012)	Min: 2.46×10^6 m^3/a, max: 5.47×10^7 m^3/a
Monthly precipitation	Data from a dataset of monthly values of climate data from the Miyun Station in China meteorological data service centre	Mean annual precipitation 633 mm/a (2007-2017)
Hydrogeological zones, and K, S_s, S_y, n, α values	(Zheng et al., 2015)	Adjusted during the calibration process
Groundwater table	14 monitoring wells in the unconfined aquifer. Data provided by BWSTI.	All wells are monitored one time per month. Partially clogged wells are no data in some months.
Cl^- and NO_3-N concentration	14 monitoring wells in the unconfined aquifer. Data provided by BWSTI.	Each well was sampled from 3 to 4 times per year.

2.4 Numerical modeling

2.4.1 Groundwater flow and solute transport modeling

Numerical simulations of groundwater flow and solute transport in this study area were performed using MODFLOW (McDonald and Harbaugh, 1988) and MT3DMS (Zheng et al., 2012) codes, respectively, under the visual MODFLOW software (WHI, 2011). The simulation period was December 2007 to December 2027 with a monthly stress period. The model was conducted with a total simulation time of 241 months, as stress periods. The model domain was discretized into 150 columns and 170 rows with a grid size of 100 m × 100 m. The total thickness of the aquifer system is 200 m including four aquifers and three aquitards (Fig. 1b). The aquifer system was divided into seven model layers to represent each aquifer and

aquitard. The top surface elevation was determined using the Digital Elevation Model (DEM). The bottom of each layer was generated by interpolating the boreholes data. Further analysis and discussion in this study focus on the unconfined aquifer (first layer) due to this aquifer has been significantly affected by RW relative to other aquifers.

According to the monitoring data on the groundwater levels of monitoring wells, the no-flow boundary was applied to the northern boundary AB and the general head boundary applied to the eastern boundary BC and western boundary AD (Fig. S1a). The south boundary CD was characterized by a constant head boundary. The top boundary was the free surface of the unconfined aquifer. The lowest boundary is the bottom of the seventh layer, most of which are limestone and dolomite with low permeability (4.6×10^{-11}~1.2×10^{-9} of hydraulic conductivity) (Louis, 1972). This boundary is generalized to the confining boundary.

Water fluxes across the top boundary include recharge from the precipitation infiltration, leakage recharge from the river channel, and discharge through the leakage of the unconfined aquifer and evaporation. Recharge from precipitation is calculated as the product of the monthly values of precipitation in the period 2007–2017 and the local precipitation infiltration coefficient (Fig. S1b) (Zheng, 2012). The river leakage recharge, including the Chaobai River and Jian River, was calculated through water balance in the river channel:

$$Q_R = Q_{RW}+Q_P - Q_E - Q_T \quad (1)$$

where Q_R is the river leakage recharge, Q_{RW} is RW transfer volume, Q_P is precipitation recharge, Q_E is evaporation from the water surface, Q_T is the transferred river water to upstream, and the unit is m^3/a.

Due to RW restoring the river channel formed a large surface water area (approximately 5.63 km^2), river leakage recharge was regarded as planar recharge, the same as precipitation infiltration. The temporal recharge rate in the upper layer can be estimated as a combination of rainfall and river leakage. Groundwater is mainly pumped from the aquifers below 80 m depth. The well fields were simulated as pumping wells, and their discharge rates were assigned on the fifth and seventh layers. The amount of groundwater evaporation was very small due to the low groundwater table. When the groundwater table depth in the North China Plain is greater than 3 m, evaporation of the unconfined groundwater disappears (Huo, 2015). Thus, the evaporation was simulated in the zones where the groundwater table depth is shallower than 3 m. The observed groundwater levels in the unconfined aquifer and the confined aquifers at the end of 2007 were interpolated as the initial groundwater levels.

The solute transport model was developed based on the groundwater flow model. Cl^- as a conservative solute has been generally used to trace and evaluate the impact of RW recharge on subsurface flow systems (Yu et al., 2016; Zhang and Yu, 2021). Cl^- concentrations of RW are usually higher than that in natural water.

The Cl^- concentration in the unconfined groundwater increased after RW restoring the river channel. Besides RW, industrial pollution in the study area is also the source of Cl^- inputting into groundwater. But the latter didn't affect the unconfined groundwater surrounding the monitoring wells except G32 (He et al., 2021). The high Cl^- concentrations in the unconfined groundwater along the river are mainly affected by the RW infiltration. Thus, the river leakage was assumed to be the only source of high concentrations of Cl^- in the model. The river was treated as a constant concentration boundary condition with Cl^- concentration of 60~120 mg/L according to the observed values. The observed data at the end of 2007 was interpolated to be the initial Cl^- concentrations. The Cl^- concentrations in rainfall and lateral flow can be set as 2 mg/L (Gao et al., 2015).

The study area is divided into various parameter zones(Fig. S1c)with different layers. The initial values of hydraulic conductivity (K), storage coefficient (S_s) specific yield (S_y), porosity (n), and dispersion coefficient (a) can be obtained from the previous work done by Zheng et al. (2015) in the study area.

2.4.2 Model calibration and validation

The model was calibrated by trial-and-error method based on the groundwater table and the Cl^- concentrations of observation wells from December 2007 to December 2015. The validation period ranges from January 2016 to December 2017. The root means squared error (RMSE) (Eq. 2) and the coefficient of determination (R^2) (Eq. 3) were used to evaluate the goodness-of-fit of the calibrated model.

$$RMSE = \sqrt{\frac{1}{n}\sum_{n}^{i=1}(O_i - S_i)^2} \quad (2)$$

$$R^2 = \frac{\left(\sum_{n}^{i=1}(O_i - O_m)(S_i - S_m)\right)^2}{\sum_{n}^{i=1}(O_i - O_m)^2 \sum_{n}^{i=1}(S_i - S_m)^2} \quad (3)$$

where n is the number of observation points, O_i is the ith observed data, S_i is the ith simulated result, and O_m is the mean value of observed data.

2.4.3 Scenario design

Six modeling scenarios were designed based on different conditions to predict groundwater changes and analyze the influences of precipitation, groundwater extraction, and RW recharge (Table 2). A baseline scenario was designed to compare the modeling results of different scenarios. Then, the groundwater dynamics in the next 10 years after 2017 were predicted using the calibrated numerical model.

Table 2
Scenario design for the groundwater model in the study area

Scenario ID	Precipitation [a]	Groundwater extraction [b]	RW recharge [c]
Baseline scenario	2007–2017 series	2017	Yes
1	1993 (dry year)	2017	Yes
2	2005 (normal year)	2017	Yes
3	1982 (wet year)	2017	Yes
4	2007–2017 series	25% reduction	Yes
5	2007–2017 series	25% increase	Yes
6	2007–2017 series	2017	No

[a] "2007–2017 series" means the monthly precipitation from 2018 to 2027 repeats the monthly precipitation series from 2007 to 2017. "1993 (dry year)" means the monthly precipitation from 2018 to 2027 repeats the monthly precipitation in1993. And so on, for 2005 (normal year) and 1982 (wet year).

[b] "2017" means the groundwater extraction volume in all well fields from 2018 to 2027 is the same as the groundwater extraction volume in 2017. "25% reduction (increase)" means the groundwater extraction volume of the well field A from 2018 to 2027 is decreased (increased) by 25% compared with 2017.

[c] "Yes" means RW recharge from 2018 to 2027 remains unchanged, the same as in 2017. "No" means there is no RW recharge from 2018 to 2027.

Climate change affects the hydrological cycle through changes in precipitation and the occurrence of extreme weather. Different annual and seasonal precipitation level changes, the frequency and intensity of floods and droughts, would affect the groundwater system (Schoenheinz and Grischek, 2011). However, it is difficult to predict the precipitation in the next 10 years based on the existing meteorological data. Therefore, it is necessary to assume multiple data-sets reflecting different precipitation trends for prediction. Based on the monthly precipitation data of the Miyun Station from 1956 to 2020, 1993, 2005, and 1982 were selected to represent the dry, normal, and wet year, respectively. Accordingly, the annual precipitation for the 10 years of model prediction period (2018-2027) was 454.8 mm, 574.6 mm, and 710.9 mm, respectively.

Beijing has taken a series of measures to restrict groundwater exploitation (State Council of the People's Republic of China, 2014). The extraction volume of groundwater in the well field A has been halved since 2014. Therefore, two different groundwater exploitation scenarios were set up to discuss the impact of groundwater exploitation on the RW infiltration in the study area. Based on the extraction volume (2.7×10^7 m^3/a) of the well field A in 2017, the designed extraction volume of groundwater of the well field A in the next 10 years will increase by 25% or decrease by 25% in different scenarios.

RW infiltration is an important recharge source for groundwater around the river channel. A scenario was set up as no RW recharge in the next 10 years (2018-2027). Compared the difference with or without RW recharge to discuss the impact of RW recharge on surrounding groundwater.

2.5 Estimation of Cl^- and NO_3-N loads in the unconfined aquifer

The pollutant load can be calculated from the groundwater storage and pollutant concentration for a given area, reflecting the changes in groundwater pollution under the combined effect of groundwater quantity and quality (Su et al., 2019; Kang et al., 2021). In this study, the concentration gradient was not considered. The formula is as follows:

$$P = \sum_{n}^{i=1} C_i S_i \quad (4)$$

where P refers to the Cl^- or NO_3-N loads, C_i is the solute concentration of the groundwater in the i cell (mg/L), and S_i is groundwater storage in the i cell (m^3).

The groundwater table and Cl^- concentration of each cell can be obtained from the modeling results. The NO_3-N concentration of each cell can be gained by interpolating the observed NO_3-N concentrations in the discrete grids of the model.

3 Results

3.1 Groundwater model calibration and validation

The RW mainly infiltrates into the unconfined aquifer along the river channel. The average proportion of RW in the unconfined aquifer is the highest of all aquifers from 2007 to 2018, reaching up to 53% (He et al., 2021). The unconfined aquifer is significantly affected by reclaimed water recharge in groundwater level (Zheng et al., 2015; He et al., 2021), hydrochemistry (Li et al., 2019; Jiang et al., 2020), and water quality (Li et al., 2013a; Ma et al., 2015; Wang et al., 2019). This study focuses on the unconfined aquifer.

The parameters of the first layer of groundwater flow and solute model were calibrated and validated with the history matching. First, the parameters need to be adjusted for minimizing the difference between the observed and simulated outputs. Four typical wells distributed along the bank of recharged river channel from upstream to downstream were selected to represent the groundwater table around the perennial and intermittent water-receiving river channel. Fig. 2 presents the fitted results for the simulated groundwater table and Cl^- concentrations in 4 typical observation wells of the unconfined aquifer. During the calibration and validation periods, the RMSE value was 0.35 m, and the R^2 value was 0.99 for the groundwater table, and the RMSE value was 11.9 mg/L, and the R^2 value was 0.68 for Cl^- concentrations,

respectively. It indicates that the model can be used to predict the variations of the groundwater table and simulate Cl^- transport in the aquifer. The zonations of the layers are shown in Fig. S1b. The calibrated parameters of the layers referenced from Zheng et al. (2015) and are shown in Table S1.

3.2 Changes of the groundwater table and the unconfined groundwater storage

3.2.1 Changes in the groundwater table

Figure 3 shows the simulated results of the groundwater level at the end of 2008, 2009, 2012, and 2017 after RW restoring the river channel. The area with the lowest groundwater table is located in the north of the Xiangyang sluice. The groundwater tables were still falling during the 10 years (2007–2017) after RW recharge, along with groundwater exploitation. The groundwater table in the south of the Xiangyang sluice increased quickly, around 3 m after the RW recharge for two years (2007–2009). The closer to the river, the more significant the groundwater table rises due to the RW infiltration.

3.2.2 Groundwater budget analysis

The groundwater budget of the unconfined aquifer was summarized in Table 3. The total recharge and discharge volume during the simulation period (Dec. 2007–Dec. 2017) was 8.94×10^8 m^3 and 10.23×10^8 m^3, respectively, with a reduction in groundwater volume of 1.29×10^8 m^3. The main recharge sources are precipitation infiltration, lateral inflow, and RW infiltration. The amount of precipitation infiltration was 7.56×10^8 m^3 in the simulation period, accounting for 84.6% of the total recharge. The amount of RW infiltration was 5.9×10^7 m^3 (6.7%). For discharge items, the leakage of the unconfined aquifer was 9.97×10^8 m^3 (97.4%), which was greater than the total recharge. The groundwater table of the unconfined aquifer was higher than those of the first and second confined aquifers. An increase in the vertical hydraulic gradient due to the deep groundwater pumping enhanced the RW infiltration into the deep aquifers. In contrast, the lateral outflow and evaporation were 2.3×10^7 m^3 (2.2%) and 4×10^6 m^3 (0.4%). They accounted for a small part of the total discharge volume. Therefore, the discharge leakage of the unconfined aquifer driven by the deep groundwater withdrawal was responsible for the negative balance of the unconfined groundwater storage.

Table 3
The unconfined groundwater budget from Dec. 2007 to Dec. 2017

Recharge items	Volume (10^8 m^3)	Proportion [a]	Discharge items	Volume (10^8 m^3)	Proportion [a]
Precipitation infiltration	7.56	84.6%	Leakage	9.97	97.4%
Lateral flow	0.78	8.7%	Lateral flow	0.23	2.2%
RW infiltration	0.59	6.7%	Evaporation	0.04	0.4%
Leakage	0.01	0.1%			
Total input	8.94		Total output	10.23	100.0%
Storage change			-1.29		

[a] "Proportion" means the proportion of recharge (discharge) items in total input (output)

3.3. Variations of the Cl^- concentrations

Figure 4 shows contour maps of the simulated Cl^- concentrations at the end of 1st, 2nd, 5th, and 10th years after RW restoring the river channel. The Cl^- concentrations in the unconfined groundwater increased from 5~75 mg/L to 50~130 mg/L from the end of 2007 to 2010, and then remained stable (Fig. 2d). The groundwater Cl^- concentrations in this area decrease with the increasing distance from the river channel. Both precipitation infiltration and subsurface lateral flow played a dilutive effect, the Cl^- concentration in the areas away from the river channel was gradually decreased.

4 Discussion

4.1 Effect of different recharge and discharge conditions on the groundwater system

The difference of the modeling results in groundwater Cl^- concentration under different precipitation scenarios is small than 10 mg/L. The prediction results show that Cl^- concentrations in the unconfined groundwater could be rapidly diluted without RW recharge as RW is the only source of high concentrations of Cl^- in the model. There is almost no difference in the modeling results in Cl^- concentration under different groundwater extraction scenarios. Therefore, only the influence of different scenarios on the groundwater table will be discussed below.

Precipitation infiltration as the main source of recharge for unconfined groundwater affects the variations of groundwater levels. In different precipitation scenarios, the groundwater table in wet scenario > baseline scenario > normal scenario > dry scenario (Fig. S2). The interannual variation of the groundwater

table under the baseline scenario is the smallest, approximated as a state of balance. Long-term low rainfall will cause the groundwater table to drop. In Fig. S2d, we can see that the groundwater table in the wet scenario is up to 2 m and 4 m higher than in the normal and dry scenarios, respectively, after 10 years.

The scenarios with baseline precipitation and RW recharge (scenarios 4 and 5) demonstrated the impact of groundwater exploitation. Fig. S3 shows the groundwater table under different groundwater extraction scenarios. The results show that the reduction in groundwater withdrawal can recover the groundwater table. The closer to the well field, the greater the groundwater table changes affected by groundwater extraction. For example, the well G01 closest to the well field has a maximum groundwater table amplitude of ~ 2 m between the increase and reduction scenarios (Fig. S3a).

The scenario of baseline precipitation and groundwater extraction (scenario 6) was designed to demonstrate the influence of RW recharge. Compared with the baseline scenario, the groundwater table dropped when there was no RW recharge and then reached a relatively stable state. The difference in groundwater table with and without RW recharge is about 3m, 5m, 11m, and 5m at G01, G15, G22, and G30, respectively (Fig. S4). It indicates that the continuous RW recharge helps maintain the groundwater table stable. When there is no RW recharge, the groundwater table around the river channel will reduce to a low level.

4.2 Variations of the unconfined groundwater storage

The unconfined groundwater storage can be calculated by the simulated groundwater table each year at the end of December (Fig. 5). The storage decreased year by year from 4.83×10^8 m^3 at the end of 2007 to 3.88×10^8 m^3 at the end of 2011. Although the groundwater table around the river has risen after the RW recharged, the groundwater table in the north Xiangyang sluice has been falling due to the continuous groundwater exploitation. Since 2012, the section between Henan rubber dam and Suzhuang rubber dam has been replenished by the RW. The storage increased to 4.1×10^8 m^3 by the end of 2012, then continued to decline and was up to 3.76×10^8 m^3 at the end of 2014 (Fig. 5).

In December 2014, the South-to-North Water Diversion Project began to transfer water to Beijing. The amount of groundwater extraction in the well field, which is located in the north of the Xiangyang sluice, has been halved. The declining trend of the confined groundwater level has slowed down. Moreover, the annual average leakage of the unconfined aquifer has decreased from 1.04×10^8 m^3/a (2008–2013) to 8.81×10^7 m^3/a (2014–2017). Due to the continuous RW infiltration and the groundwater extraction reduction, storage began to rise slowly since 2014. It rose from 3.76×10^8 m^3 at the end of 2014 to 3.85×10^8 m^3 at the end of 2017 (Fig. 5).

4.3 Distribution of the unconfined groundwater-affected by the RW infiltration

The increase of Cl^- concentrations may reflect the impact of RW infiltration on groundwater. The zones where the Cl^- concentration is higher than the initial concentration (5~75 mg/L) after RW recharge is defined as being affected by RW infiltration. Fig. 6 shows zones of the unconfined groundwater quality affected by RW for the 1st, 2nd, 5th, and 10th years after RW restoring the river channel. The Cl^- transport is controlled by both the groundwater flow rate and the concentration gradient. In the early stage of reclaimed water replenishment, the groundwater table elevated rapidly due to the RW infiltration, resulting in quick Cl^- movement with the groundwater flow. Thus, the zones affected by RW are distributed at both sides of the river. Due to the unconfined groundwater flows from southwest to northeast, the affected zone of the left bank is more extensive than that at the right bank (Fig. 6). The affected zones gradually expanded with the increase of time and recharged channels, but the annual increasing rate of the area decreased year by year (Table 4). It indicates that Cl^- movement slowed down with the groundwater table stable around the river.

Table 4
Variations of the zones affected by RW infiltration for the unconfined groundwater

Year	2008	2009	2010	2011	2012	2013	2014	2015	2016	2017
Area (km^2)	11.7	14.9	16.4	17.8	22.2	23.3	24.6	25.7	26.4	26.7
Increasing rate (%)		27.4	9.8	8.8	24.5	5.3	5.3	4.6	2.5	1.4

4.4 Variations of the Cl^- and NO_3-N loads

4.4.1 Cl^- loads in the unconfined groundwater

The Cl^- loads in the model area were decreased annually, dropped from 1.66×10^4 t at the end of 2007 to 3.85×10^3 t at the end of 2017 (Fig. 5). In contrast, the Cl^- loads in the affected zones rose from 1.8×10^3 t at the end of 2008 to 3.8×10^3 t at the end of 2017. There are rising trends both in the Cl^- concentrations, and Cl^- loads of the unconfined groundwater in the affected zones. The zone can represent where the unconfined groundwater quality is affected by RW in terms of solute concentration and corresponding loads.

4.4.2 NO_3-N loads in the affected zones

NO_3-N is the typical contaminant in the RW (Pan et al., 2018; Li et al., 2019). Although NO_3-N has been partially removed during the RW infiltration process, NO_3-N from the RW still enters the groundwater (Li et al., 2019). The observed NO_3-N concentrations of some monitoring wells occasionally exceed 10 mg/L (guideline for drinking water recommended by WHO (World Health Organization, 2017)). Furthermore, the change trends of groundwater NO_3-N concentrations during monitoring periods were consistent with those of groundwater Cl^- concentrations, being affected by seasonal precipitation and temperature changes (Li, 2020).

Figure 5 shows the calculated groundwater NO_3-N loads within the affected zones at the end of each year, declining from 29.8 t at the end of 2008 to 11.9 t at the end of 2017. It indicates that the RW infiltration did not increase the NO_3-N loads in the unconfined groundwater.

Although the maximum NO_3-N concentration in the RW is as high as 20.2 mg/L, the unconfined groundwater has been subjected to denitrification during the RW infiltration, especially in the south of the Xiangyang sluice (Liu et al., 2018). Denitrification hotspots are easily formed during surface water infiltration (Rivett et al., 2008; Ranalli and Macalady, 2010; Trauth et al., 2018). The attenuation rate of NO_3-N near the monitoring well G22 can reach 99.6% (Li et al., 2019).

There was a high level (48.8 t) of NO_3-N loads at the end of 2011. The NO_3-N contents near the Xiangyang sluice are relatively high due to the existing thick gravel layer, which is not conducive to remove NO_3-N (Xiong, 2009). The north channel of the earth dam has been replenished only in May and October. Sediments can adsorb NH_4-N during the wet period, which can be converted by nitrification reaction into NO_3-N during the dry period (Böhlke et al., 2006). Therefore, the unconfined groundwater near the intermittent water-receiving channel appeared high NO_3-N concentrations (~ 14.7 mg/L).

4.5 Environmental implications for management of a river channel recharged by RW

RW has been used to restore the Chaobai River, while the unconfined aquifer near the river channel was unintentionally recharged. It can be considered as a riverbank filtration (RBF) system, a way of anthropogenic aquifer recharge (AAR) (Todd, 1959; Morel-Seytoux, 1985; Dillon, 2005; NRMMC et al., 2009; Maliva, 2020a). As a result, the RW infiltration affects the groundwater level and quality around the river channel, especially the unconfined groundwater.

The RW infiltration has quickly replenished the unconfined groundwater, resulting in the groundwater table around the river channel to rose rapidly by 3~4 m in the first two years (2007–2009) (Zheng et al., 2015; He et al., 2021). However, increased recharge via the RW infiltration may not necessarily result in a corresponding increase in the groundwater storage volume (Maliva, 2020b). According to the calculated results of the unconfined groundwater storage in this study, it is necessary to combine the increase RW

recharge and reduction extractions to sustain the groundwater storage. Increasing recharge in isolation may not solve the problem of groundwater over-extraction (Gale et al., 2006; Foster and Garduño, 2013).

Water quality issues are usually the most concern in the RW utilization. The infiltration process driven by natural filtration and groundwater pumping improves or degrades the recharged water quality. It depends on the quantity and hydrochemical characteristics of RW and native groundwater, and the geochemical processes occurring during RW passes via riverbed and underlying aquifer (Ray, 2008; Stuyfzand, 2011; Tyagi et al., 2013; Hu et al., 2016). In the study area, the subsurface hydrochemistry might be modified by mixing the infiltrated RW with native groundwater and potential water-rock interactions, especially the mixing process and cation exchange (Yu, 2013; Liu et al., 2018). The hydrochemical type of the unconfined groundwater has changed from HCO_3-Ca·Mg into HCO_3·Cl-Na·Ca, which is the RW type (Li et al., 2019; Jiang et al., 2020). The hydraulic travel time of RW infiltration into the 30 m depth was about 6.5 months (Li et al., 2019). The average proportion of the RW in the unconfined aquifers is about 53% from 2007 to 2018 (He et al., 2021). NO_3-N in the RW was well attenuated with an attenuation rate of 99.6% during infiltration (Li et al., 2019). Some emerging contaminants have been detected in the unconfined groundwater from this area, such as endocrine-disrupting compounds (Li et al., 2013a; Ma et al., 2015) and antibiotics and antibiotic resistance genes (Zhang et al., 2018).

Although the RW recharge to a river channel may inevitably affect the groundwater quality of the underlying aquifers, the affected zones are limited. In the affected zones, the Cl^- loads of the unconfined groundwater were increased and NO_3-N loads of the unconfined groundwater attenuated in the zones. But outside of these affected zones, the groundwater quality is characterized by the initial concentration of the aquifer.

RW utilization for recharging the river channel and the ambient groundwater system is usually a double-edged sword, which can bring the environment both benefits and harms. The main benefits are restoring the riverine ecosystem, increasing and maintaining the groundwater table and storage, and reducing groundwater pumping. At the same time, the disadvantage lies in the potential deterioration of groundwater quality, which depends on the inputs. attenuation of contaminants, and potential water-rock interaction in river-aquifer systems. Where conditions are hydro-geologically favorable, RW recharge to the river channel can be a valuable way of alleviating water shortages (Maliva, 2020a). It is important and necessary to investigate and evaluate whether the field is suitable for RW recharge (Alam et al., 2021). Based on the numerical modeling, this study shows that apart from the affected zones, the RW has lesser environmental impacts of RW infiltration on groundwater quality. In future work, we should pay more attention to variations of water quality after RW recharge, and take necessary measures to manage RW recharge. It is an essential aspect of ensuring the safe use of RW. Additionally, as the unconfined groundwater table rise, a threshold of water level should be set to prevent soil salinization in the RW receiving area.

5 Conclusions

Since the operation of the Beijing Municipal Water Diversion Project in 2007, it has been more than ten years since the implementation of reclaimed water supply to the Chaobai River, resulting in some environmental effects (e.g. groundwater level rise and water quality change). Based on long time-sequenced groundwater monitoring data, this study established a three-dimensional groundwater flow and solute transport model to evaluate the impact of the RW recharge on the groundwater table and storage change, and Cl^- and NO_3-N loads in the unconfined aquifer. Seven scenarios are designed to reveal the influence of different precipitation, groundwater extraction, and RW recharge conditions on the unconfined groundwater system.

The results show that the groundwater table around the river channel rose by about 3~4 m from Dec. 2007 to Dec. 2009 after RW recharge and then remained stable. The groundwater exploitation caused the declining groundwater table near the well field in the north of the Xiangyang sluice, and the unconfined groundwater was in a negative equilibrium state from Dec. 2007 to Dec. 2017. The continuous recharge of RW and the reduced groundwater exploitation increased the unconfined groundwater storage. Reducing the amount of groundwater exploitation by 25% can increase the surrounding groundwater table by ~1 m in 10 years (2018–2027). Stop supplying reclaimed water, and the unconfined groundwater table around the river channel will drop by ~5 m in 10 years (2018–2027).

The range of Cl^- concentrations in the unconfined groundwater significantly increased from 5~75 mg/L before RW recharge to 50~130 mg/L due to the RW infiltration. The affected zones can be identified by the increase of Cl^- concentration. The RW-affected area increased from 11.7 km^2 in 2008 to 26.7 km^2 in 2017. The affected zones tend to be annually stable with a steady RW supply. The Cl^- loads of the unconfined groundwater in the affected zones were increased annually, but the NO_3-N loads were decreasing as a whole due to NO_3-N attenuated in the zones.

In general, the river channel recharged by RW in the study area is beneficial to increase and maintain the groundwater table and the groundwater storage with lesser environmental impacts. To a large extent, the pressure on water demand in Beijing has been relieved. It suggests that long-term monitoring of surface and groundwater quality around the river channel can be implemented to keep a watchful eye on changes in groundwater quality and environmental impacts. Improving the RW quality and optimizing replenishment plans through modeling are recommended for water management around the river channel recharged by RW. In order to minimize the negative environmental effects, it is necessary to regulate the water quality and quantity in the long run to realize the optimal utilization of reclaimed water.

Declarations

Ethics approval and consent to participate

Not applicable.

Consent for publication

Not applicable.

Availability of data and materials

The datasets used and analysed during the current study are available from the corresponding author on reasonable request.

Competing interests

The authors declare that they have no competing interests.

Funding

This research was funded by the Beijing Municipal Natural Science Foundation (Grant No. 8212035) and the National Natural Science Foundation of China (Grant No. 41730749).

Authors' contributions

Conceptualization: Ruixue Jiang, Dongmei Han, Xianfang Song and Fandong Zheng; Formal analysis, Software, and Visualization: Ruixue Jiang, Dongmei Han; Investigation: Ruixue Jiang, Dongmei Han and Fandong Zheng; Funding acquisition: Xianfang Song, Dongmei Han; Resources: Xianfang Song, Dongmei Han and Fandong Zheng; Supervision: Dongmei Han, Xianfang Song; Writing - original draft preparation: Ruixue Jiang, Dongmei Han; Writing - review and editing: Ruixue Jiang, Dongmei Han and Xianfang Song.

Acknowledgements

We are grateful for Dr. Zhao Zhanfeng’s help in setting up the model.

References

1. Ahuja S (2015) Overview of Global Water Challenges and Solutions, in: Water Challenges and Solutions on a Global Scale, ACS Symposium Series. American Chemical Society, pp. 1–25. https://doi.org/10.1021/bk-2015-1206.ch001
2. Aji K, Tang C, Song X, Kondoh A, Sakura Y, Yu J, Kaneko S (2008) Characteristics of chemistry and stable isotopes in groundwater of Chaobai and Yongding River basin, North China Plain. Hydrol Process 22:63–72. https://doi.org/10.1002/hyp.6640

3. Alam S, Borthakur A, Ravi S, Gebremichael M, Mohanty SK (2021) Managed aquifer recharge implementation criteria to achieve water sustainability. Science of The Total Environment 768:144992. https://doi.org/10.1016/j.scitotenv.2021.144992
4. Angelakis AN, Asano T, Bahri A, Jimenez BE, Tchobanoglous G (2018) Water Reuse: From Ancient to Modern Times and the Future. Front Environ Sci 6:26. https://doi.org/10.3389/fenvs.2018.00026
5. Angelakis AN, Gikas P (2014) Water reuse: Overview of current practices and trends in the world with emphasis on EU states. Water Utility Journal 8:67–78
6. Asano T (2007) Water reuse: issues, technologies, and applications. McGraw-Hill, New York
7. Asano T, Cotruvo JA (2004) Groundwater recharge with reclaimed municipal wastewater: health and regulatory considerations. Water Res 38:1941–1951. https://doi.org/10.1016/j.watres.2004.01.023
8. Beijing Water A (2020) Beijing Water Resources Bulletin (2019). Beijing Water Authority, Beijing
9. Beijing Water A (2019) Beijing Water Statistical Yearbook (2018). Beijing Water Authority
10. Bekele E, Page D, Vanderzalm J, Kaksonen A, Gonzalez D (2018) Water Recycling via Aquifers for Sustainable Urban Water Quality Management: Current Status, Challenges and Opportunities. Water 10:457. https://doi.org/10.3390/w10040457
11. Bekele E, Toze S, Patterson B, Higginson S (2011) Managed aquifer recharge of treated wastewater: Water quality changes resulting from infiltration through the vadose zone. Water Res 45:5764–5772. https://doi.org/10.1016/j.watres.2011.08.058
12. Böhlke JK, Smith RL, Miller DN (2006) Ammonium transport and reaction in contaminated groundwater: Application of isotope tracers and isotope fractionation studies. Water Resour Res 42. https://doi.org/10.1029/2005WR004349
13. Daesslé LW, Andrade-Tafoya PD, Lafarga-Moreno J, Mahlknecht J, van Geldern R, Beramendi-Orosco LE, Barth JAC (2020) Groundwater recharge sites and pollution sources in the wine-producing Guadalupe Valley (Mexico): Restrictions and mixing prior to transfer of reclaimed water from the US-México border. Science of The Total Environment 713:136715. https://doi.org/10.1016/j.scitotenv.2020.136715
14. Davranche M, Bollinger J-C (2000) Heavy Metals Desorption from Synthesized and Natural Iron and Manganese Oxyhydroxides: Effect of Reductive Conditions. J Colloid Interface Sci 227:531–539. https://doi.org/10.1006/jcis.2000.6904
15. De Gisi S, Casella P, Cellamare CM, Ferraris M, Petta L, Notarnicola M (2017) Wastewater Reuse. In: Abraham MA (ed) Encyclopedia of Sustainable Technologies. Elsevier, Oxford, pp 53–68. https://doi.org/10.1016/B978-0-12-409548-9.10528-7
16. Deng S, Yan X, Zhu Q, Liao C (2019) The utilization of reclaimed water: Possible risks arising from waterborne contaminants. Environ Pollut 254:113020. https://doi.org/10.1016/j.envpol.2019.113020
17. Dillon P (2005) Future management of aquifer recharge. Hydrogeol J 13:313–316. https://doi.org/10.1007/s10040-004-0413-6

18. Ding G, Chen G, Liu Y, Li M, Liu X (2020) Occurrence and risk assessment of fluoroquinolone antibiotics in reclaimed water and receiving groundwater with different replenishment pathways. Science of The Total Environment 738:139802. https://doi.org/10.1016/j.scitotenv.2020.139802
19. Fakhreddine S, Prommer H, Scanlon BR, Ying SC, Nicot J-P (2021) Mobilization of Arsenic and Other Naturally Occurring Contaminants during Managed Aquifer Recharge: A Critical Review. Environ Sci Technol. https://doi.org/10.1021/acs.est.0c07492
20. Foster S, Garduño H (2013) Irrigated agriculture and groundwater resources – towards an integrated vision and sustainable relationship. Water Sci Technol 67:1165–1172. https://doi.org/10.2166/wst.2013.654
21. Gale IN, Macdonald DMJ, Calow RC, Neumann I, Moench M, Kulkarni H, Mudrakartha S, Palanisami K (2006) Managed aquifer recharge: An assessment of its role and effectiveness in watershed management. British Geological Survey, Nottingham
22. Gao X, Chen X, Ding Z, Yang W (2015) Investigation of the variation of atmospheric pollutants from chemical composition of precipitation along an urban-to-rural transect in Beijing. Acta Sci Circum 35:4033–4042
23. Gilabert-Alarcón C, Daesslé LW, Salgado-Méndez SO, Pérez-Flores MA, Knöller K, Kretzschmar TG, Stumpp C (2018) Effects of reclaimed water discharge in the Maneadero coastal aquifer, Baja California, Mexico. Appl Geochem 92:121–139. https://doi.org/10.1016/j.apgeochem.2018.03.006
24. Guo X, Feng Q, Si J, Xi H, Zhao Y, Deo RC (2019) Partitioning groundwater recharge sources in multiple aquifers system within a desert oasis environment: Implications for water resources management in endorheic basins. J Hydrol 579:124212. https://doi.org/10.1016/j.jhydrol.2019.124212
25. He Z, Han D, Song X, Yang L, Zhang Y, Ma Y, Bu H, Li B, Yang S (2021) Variations of Groundwater Dynamics in Alluvial Aquifers with Reclaimed Water Restoring the Overlying River, Beijing, China. Water 13:806. https://doi.org/10.3390/w13060806
26. Hess DJ, Collins BM (2019) Recycling water in US cities: understanding preferences for aquifer recharging and dual-reticulation systems. Water Policy 21:1207–1223. https://doi.org/10.2166/wp.2019.162
27. Hu B, Teng Y, Zhai Y, Zuo R, Li J, Chen H (2016) Riverbank filtration in China: A review and perspective. J Hydrol 541:914–927. https://doi.org/10.1016/j.jhydrol.2016.08.004
28. Huo S (2015) Research on the Effect of Water Table Decline on Vertical Groundwater Recharge——A Case Study in the North China Plain (Doctor). China University of Geosciences
29. Jiang R, Han D, Song X, Yang L, Li B (2020) Impacts of reclaimed water recharge to river channel on ambient water bodies: a case study of Beijing Chaobai River. Resources Science 42:2419–2433. https://doi.org/10.18402/resci.2020.12.13
30. Kang J-H, Park M-H, Ha SJ, Stenstrom MK (2021) An empirical modeling approach to predicting pollutant loads and developing cost-effective stormwater treatment strategies for a large urban

watershed. Science of The Total Environment 760:143388. https://doi.org/10.1016/j.scitotenv.2020.143388

31. Kog YC (2020) Water Reclamation and Reuse in Singapore. J Environ Eng-ASCE 146:03120001. https://doi.org/10.1061/(ASCE)EE.1943-7870.0001675
32. Li C (2020) Analysis of Evolution Characteristics of Groundwater Quality under River Infiltration Recharge with Reclaimed Water (Master). China University of Geosciences (Beijing), Beijing
33. Li C, Li B, Bi E (2019) Characteristics of hydrochemistry and nitrogen behavior under long-term managed aquifer recharge with reclaimed water: A case study in north China. Science of The Total Environment 668:1030–1037. https://doi.org/10.1016/j.scitotenv.2019.02.375
34. Li J, Fu J, Zhang H, Li Z, Ma Y, Wu M, Liu X (2013a) Spatial and seasonal variations of occurrences and concentrations of endocrine disrupting chemicals in unconfined and confined aquifers recharged by reclaimed water: A field study along the Chaobai River, Beijing. Science of The Total Environment 450–451:162–168. https://doi.org/10.1016/j.scitotenv.2013.01.089
35. Li J, Fu J, Zhang H, Li Z, Ma Y, Wu M, Liu X (2013b) Spatial and seasonal variations of occurrences and concentrations of endocrine disrupting chemicals in unconfined and confined aquifers recharged by reclaimed water: A field study along the Chaobai River, Beijing. Science of The Total Environment 450–451:162–168. https://doi.org/10.1016/j.scitotenv.2013.01.089
36. Li Z, Xiang X, Li M, Ma Y, Wang J, Liu X (2015) Occurrence and risk assessment of pharmaceuticals and personal care products and endocrine disrupting chemicals in reclaimed water and receiving groundwater in China. Ecotoxicol Environ Saf 119:74–80. https://doi.org/10.1016/j.ecoenv.2015.04.031
37. Liu L, Shan Y, Li B, Yang Y (2018) Interaction mechanism experiment of water and rocks in infiltration of reclaimed water. Water Resources Protection 34:31–35
38. Louis C (1972) Rock Hydraulics. Rock Mechanics 299–387. https://doi.org/10.1007/978-3-7091-4109-0_16
39. Ma W, Nie C, Su F, Cheng X, Yan Y, Chen B, Lun X (2015) Migration and biotransformation of three selected endocrine disrupting chemicals in different river-based aquifers media recharge with reclaimed water. International Biodeterioration & Biodegradation, CESE-2014 – Challenges in Environmental Science and Engineering Series Conference 102, 298–307. https://doi.org/10.1016/j.ibiod.2015.03.022
40. Machiwal D, Jha MK, Singh VP, Mohan C (2018) Assessment and mapping of groundwater vulnerability to pollution: Current status and challenges. Earth Sci Rev 185:901–927. https://doi.org/10.1016/j.earscirev.2018.08.009
41. Maliva RG (2020a) Introduction to Anthropogenic Aquifer Recharge. In: Maliva RG (ed) Anthropogenic Aquifer Recharge: WSP Methods in Water Resources Evaluation Series No. 5, Springer Hydrogeology. Springer International Publishing, Cham, pp 1–20. https://doi.org/10.1007/978-3-030-11084-0_1

42. Maliva RG (2020b) Groundwater Recharge and Aquifer Water Budgets. In: Maliva RG (ed) Anthropogenic Aquifer Recharge: WSP Methods in Water Resources Evaluation Series No. 5, Springer Hydrogeology. Springer International Publishing, Cham, pp 63–102. https://doi.org/10.1007/978-3-030-11084-0_4
43. McDonald MG, Harbaugh AW (1988) A Modular Three-dimensional Finite-difference Ground-water Flow Model. U.S. Geological Survey
44. Morel-Seytoux HJ (1985) CHAPTER 3 - Conjunctive Use of Surface and Ground Waters, in: Asano, T. (Ed.), Artificial Recharge of Groundwater. Butterworth-Heinemann, pp. 35–67. https://doi.org/10.1016/B978-0-250-40549-7.50008-4
45. MWR (2021) China Water Resources Bulletin (2019). Ministry of Water Resources of the People's Republic of China
46. NRMMC EPHC, NHMRC, 2009. Water Quality Australian guidelines for water recycling: Managed Aquifer Recharge. https://www.waterquality.gov.au/guidelines/recycled-water#managing-health-and-environmental-risks-phase-1 (accessed 1 December 2019)
47. Page D, Dillon P, Toze S, Bixio D, Genthe B, Jiménez Cisneros BE, Wintgens T (2010) Valuing the subsurface pathogen treatment barrier in water recycling via aquifers for drinking supplies. Water Res 44:1841–1852. https://doi.org/10.1016/j.watres.2009.12.008
48. Pan W, Huang Q, Huang G (2018) Nitrogen and Organics Removal during Riverbank Filtration along a Reclaimed Water Restored River in Beijing, China. Water 10:491. https://doi.org/10.3390/w10040491
49. Patterson BM, Shackleton M, Furness AJ, Pearce J, Descourvieres C, Linge KL, Busetti F, Spadek T (2010) Fate of nine recycled water trace organic contaminants and metal(loid)s during managed aquifer recharge into a anaerobic aquifer: Column studies. Water Res 44:1471–1481. https://doi.org/10.1016/j.watres.2009.10.044
50. Ranalli AJ, Macalady DL (2010) The importance of the riparian zone and in-stream processes in nitrate attenuation in undisturbed and agricultural watersheds – A review of the scientific literature. J Hydrol 389:406–415. https://doi.org/10.1016/j.jhydrol.2010.05.045
51. Ray C (2008) Worldwide potential of riverbank filtration. Clean Techn Environ Policy 10:223–225. https://doi.org/10.1007/s10098-008-0164-5
52. Rivett MO, Buss SR, Morgan P, Smith JWN, Bemment CD (2008) Nitrate attenuation in groundwater: A review of biogeochemical controlling processes. Water Res 42:4215–4232. https://doi.org/10.1016/j.watres.2008.07.020
53. Schoenheinz D, Grischek T (2011) Behavior of Dissolved Organic Carbon During Bank Filtration Under Extreme Climate Conditions. In: Shamrukh M (ed) Riverbank Filtration for Water Security in Desert Countries, NATO Science for Peace and Security Series C: Environmental Security. Springer Netherlands, Dordrecht, pp 51–67. https://doi.org/10.1007/978-94-007-0026-0_4
54. Sege J, Ghanem M, Ahmad W, Bader H, Rubin Y (2018) Distributed data collection and web-based integration for more efficient and informative groundwater pollution risk assessment. Environ Model Softw 100, 278–290. https://doi.org/10.1016/j.envsoft.2017.11.027

55. Singer R, Brown S (2018) Impact of Soil Filtration on Metals, Nutrients, and Estrogenic Activity of Reclaimed Water. J Environ Qual 47:1504–1512. https://doi.org/10.2134/jeq2018.03.0109
56. State Council of the People's Republic of China (2014) Regulations on Water Supply Management of the South-to-North Water Diversion Project
57. Stuyfzand PJ (2011) Hydrogeochemical Processes During Riverbank Filtration and Artificial Recharge of Polluted Surface Waters: Zonation, Identification, and Quantification. In: Shamrukh M (ed) Riverbank Filtration for Water Security in Desert Countries. NATO Science for Peace and Security Series C: Environmental Security. Springer Netherlands, Dordrecht, pp 97–128. https://doi.org/10.1007/978-94-007-0026-0_7
58. Su Y, Li K, Liang S, Lu S, Wang Y, Dai A, Li Y, Ding D, Wang X (2019) Improved simulation–optimization approach for identifying critical and developable pollution source regions and critical migration processes for pollutant load allocation. Science of The Total Environment 646:1336–1348. https://doi.org/10.1016/j.scitotenv.2018.07.326
59. Todd DK (1959) Annotated bibliography on artificial recharge of ground water through 1954 (No. 1477), Water Supply Paper. U.S. Govt. Print. Off.,. https://doi.org/10.3133/wsp1477
60. Tortajada C, van Rensburg P (2020) Drink more recycled wastewater. Nature 577:26–28. https://doi.org/10.1038/d41586-019-03913-6
61. Trauth N, Musolff A, Knöller K, Kaden US, Keller T, Werban U, Fleckenstein JH (2018) River water infiltration enhances denitrification efficiency in riparian groundwater. Water Res 130:185–199. https://doi.org/10.1016/j.watres.2017.11.058
62. Tyagi S, Dobhal R, Kimothi PC, Adlakha LK, Singh P, Uniyal DP (2013) Studies of River Water Quality Using River Bank Filtration in Uttarakhand, India. Water Qual Expo Health 5:139–148. https://doi.org/10.1007/s12403-013-0097-z
63. USEPA USAID (2012) Guidelines for Water Reuse (No. EPA/600/R-12/618). U.S. Environmental Protection Agency, Washington, D.C.
64. Valhondo C, Carrera J, Martínez-Landa L, Wang J, Amalfitano S, Levantesi C, Diaz-Cruz MS (2020) Reactive Barriers for Renaturalization of Reclaimed Water during Soil Aquifer Treatment. Water 12:1012. https://doi.org/10.3390/w12041012
65. Wang P, Rene ER, Yan Y, Ma W, Xiang Y (2019) Spatiotemporal evolvement and factors influencing natural and synthetic EDCs and the microbial community at different groundwater depths in the Chaobai watershed: A long-term field study on a river receiving reclaimed water. J Environ Manage 246:647–657. https://doi.org/10.1016/j.jenvman.2019.05.156
66. World Health Organization (2017) Guidelines for drinking-water quality: fourth edition incorporating the first addendum. Geneva
67. WWAP (2019) The United Nations World Water Development Report 2019: Leaving No One Behind. UNESCO, Paris
68. Xiong Y (2009) The Simulated Columns Tests on the Nitrogen Transformation and Biodegradation during the Reclaimed Water Infiltration Through the Vadose (Mater). China University of Geosciences

(Beijing), Beijing

69. Yang L, He J, Liu Y, Wang J, Jiang L, Wang G (2016) Characteristics of change in water quality along reclaimed water intake area of the Chaobai River in Beijing, China. Journal of Environmental Sciences Sustainable Water Environment Water Use 50:93–102. https://doi.org/10.1016/j.jes.2016.05.023
70. Yu Y (2013) A Research of the Impact of Reclaimed Water as Scenic Water on the Groundwater in Water Channel -A Case Study of Beijing Segment of Chaobai River (Doctor). The University of Chinese Academy of Sciences
71. Yu Y, Song X, Zhang Y, Zheng F, Liu L (2016) Impact of reclaimed water in the watercourse of Huai River on groundwater from Chaobai River basin, Northern China. Front Earth Sci 11:643–659. https://doi.org/10.1007/s11707-016-0600-5
72. Yuan R, Wang M, Wang S, Song X (2020) Water transfer imposes hydrochemical impacts on groundwater by altering the interaction of groundwater and surface water. J Hydrol 583:124617. https://doi.org/10.1016/j.jhydrol.2020.124617
73. Zhang N, Liu X, Liu R, Zhang T, Li M, Zhang Z, Qu Z, Yuan Z, Yu H (2018) Influence of reclaimed water discharge on the dissemination and relationships of sulfonamide, sulfonamide resistance genes along the Chaobai River, Beijing. Front Environ Sci Eng 13:8. https://doi.org/10.1007/s11783-019-1099-2
74. Zhang R, Zhang Y, Liu L, Wang Y, Song Z, Wang X, Liu C, Li Y, Meng W, Zhou Y, Sun D, Qi F (2020) Occurrence and risk assessment of heavy metals in an urban river supplied by reclaimed wastewater. Water Environment Research wer.1341. https://doi.org/10.1002/wer.1341
75. Zhang Y, Wang J, Jing J, Sun J (2014) Response of groundwater to climate change under extreme climate conditions in North China Plain. J Earth Sci 25:612–618. https://doi.org/10.1007/s12583-014-0443-5
76. Zhang Y, Yu Y (2021) Evaluating the impact of percolated reclaimed water from river-channel reservoir on groundwater using tracers in Beijing, Northern China. Environ Earth Sci 80:138. https://doi.org/10.1007/s12665-021-09449-1
77. Zheng C, Hill MC, Cao G, Ma R (2012) MT3DMS: Model Use, Calibration, and Validation. Transactions of the ASABE 55:1549–1559. https://doi.org/10.13031/2013.42263
78. Zheng F (2012) Case Study on Effects of Reclaimed Water Use for Scenic Water on Groundwater Environment in Chaobai River (Doctor). China University of Geosciences (Beijing)
79. Zheng F, Liu L, Li B, Yang Y, Gou M (2015) Effects of Reclaimed Water Use for Scenic Water on Groundwater Environment in a Multilayered Aquifer System beneath the Chaobai River, Beijing, China: Case Study. J Hydrol Eng 20:B5014003. https://doi.org/10.1061/(ASCE)HE.1943-5584.0001052
80. Zhu Z, Dou J (2018) Current status of reclaimed water in China: an overview. Journal of Water Reuse Desalination 8:293–307. https://doi.org/10.2166/wrd.2018.070

Figures

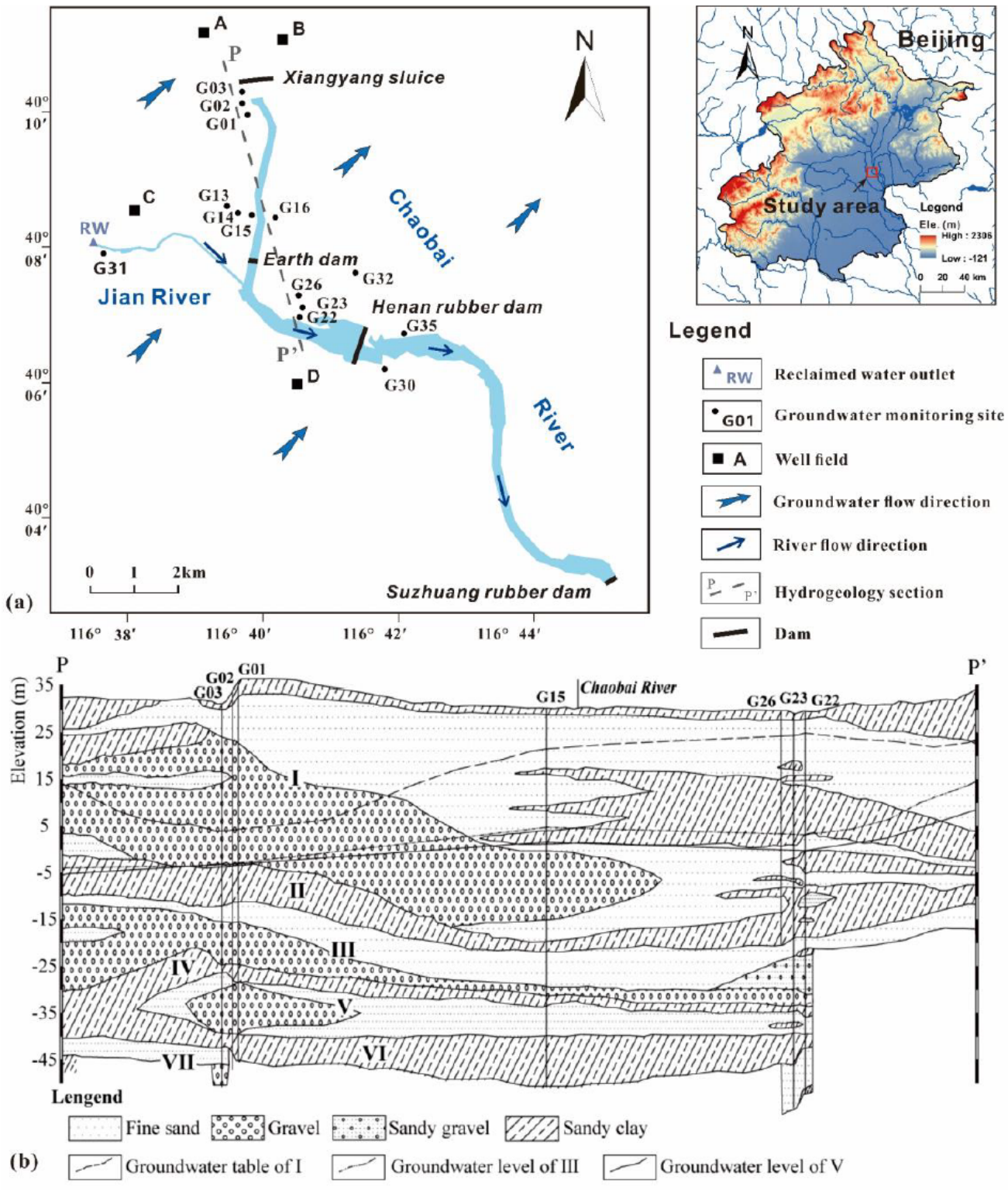

Figure 1

Location map showing (a) water sampling sites, well fields in the study area, and (b) hydrogeological cross-section along P-P' from north to south (modified from Zheng et al., 2015). I refers to the unconfined aquifer in this study, and confined aquifers refer to III, V, and □. □, □, and □ correspond to the aquitards.

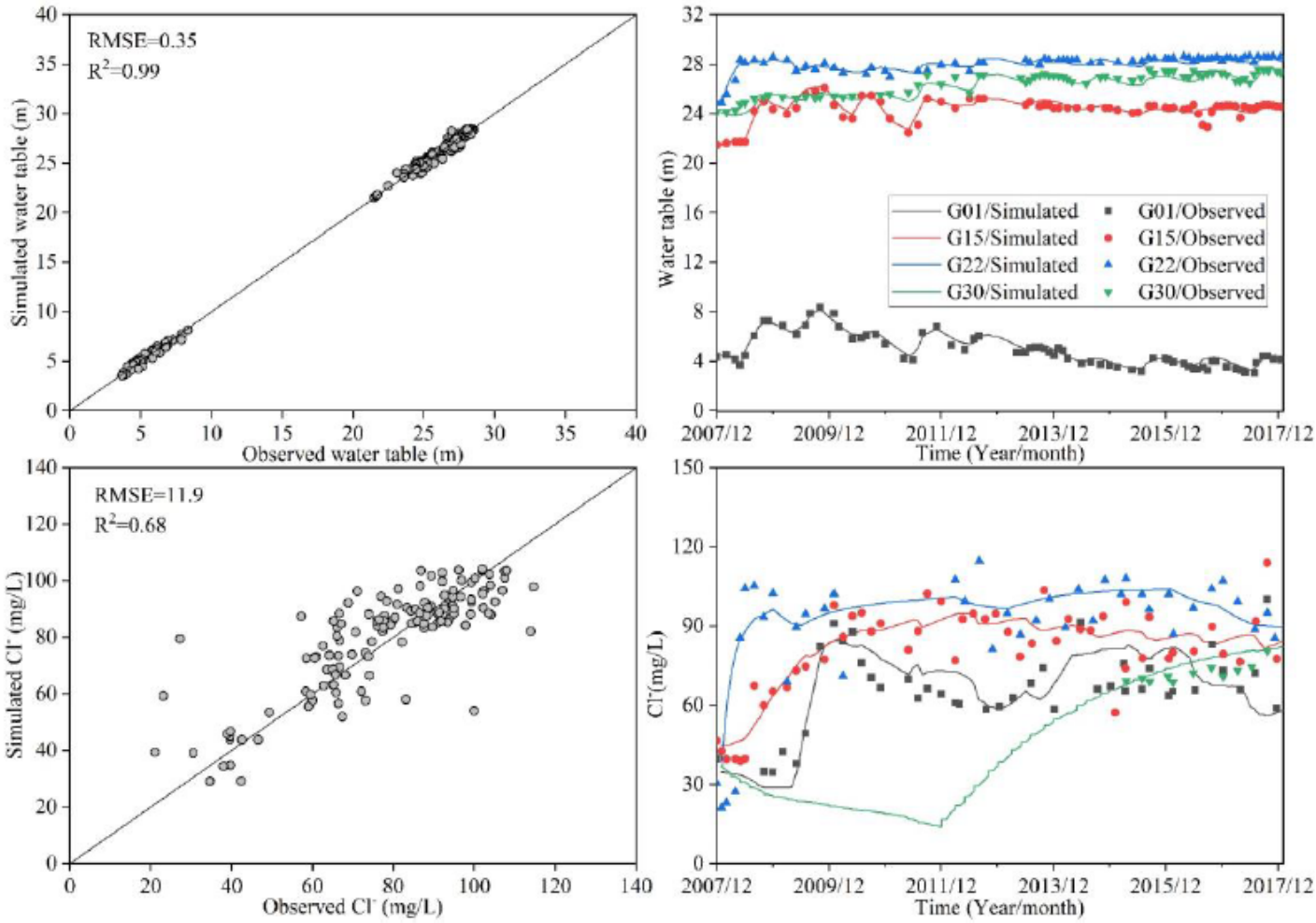

Figure 2

(a) Simulated versus observed results for groundwater tables in the unconfined aquifer, (b) comparison between the observed and simulated monthly groundwater tables for four typical observations, (c) Simulated versus observed Cl- concentration in the unconfined aquifer, (d) comparison between the observed and simulated monthly Cl- concentration for four typical observations during calibration and validation periods in the study area

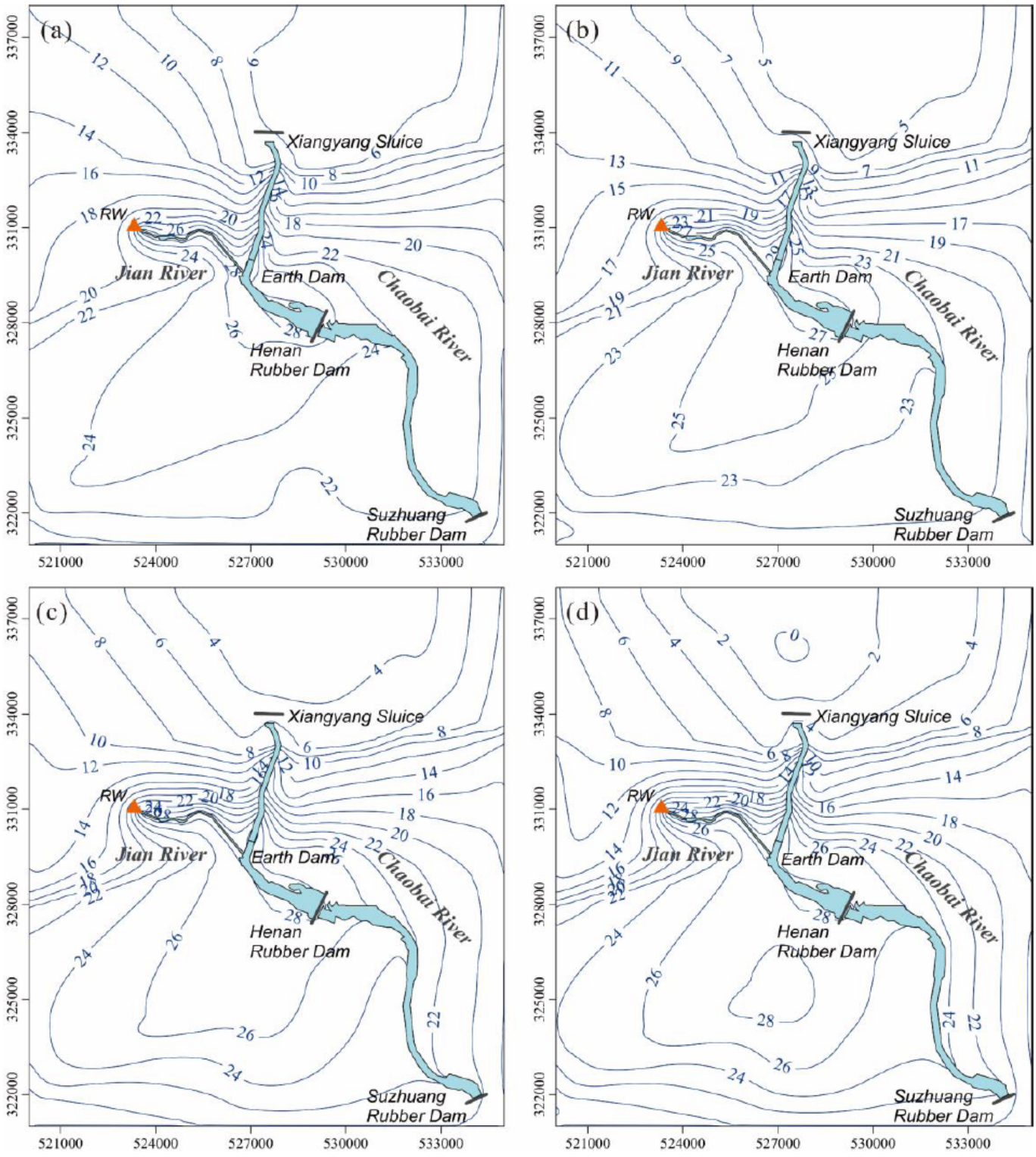

Figure 3

Distribution of the simulated groundwater table contours (unit: m) in the unconfined aquifer at the end of (a)2008, (b)2009, (c) 2012, and (d) 2017 after the RW restoring river channel (the coordinate system is the Beijing local coordinate system)

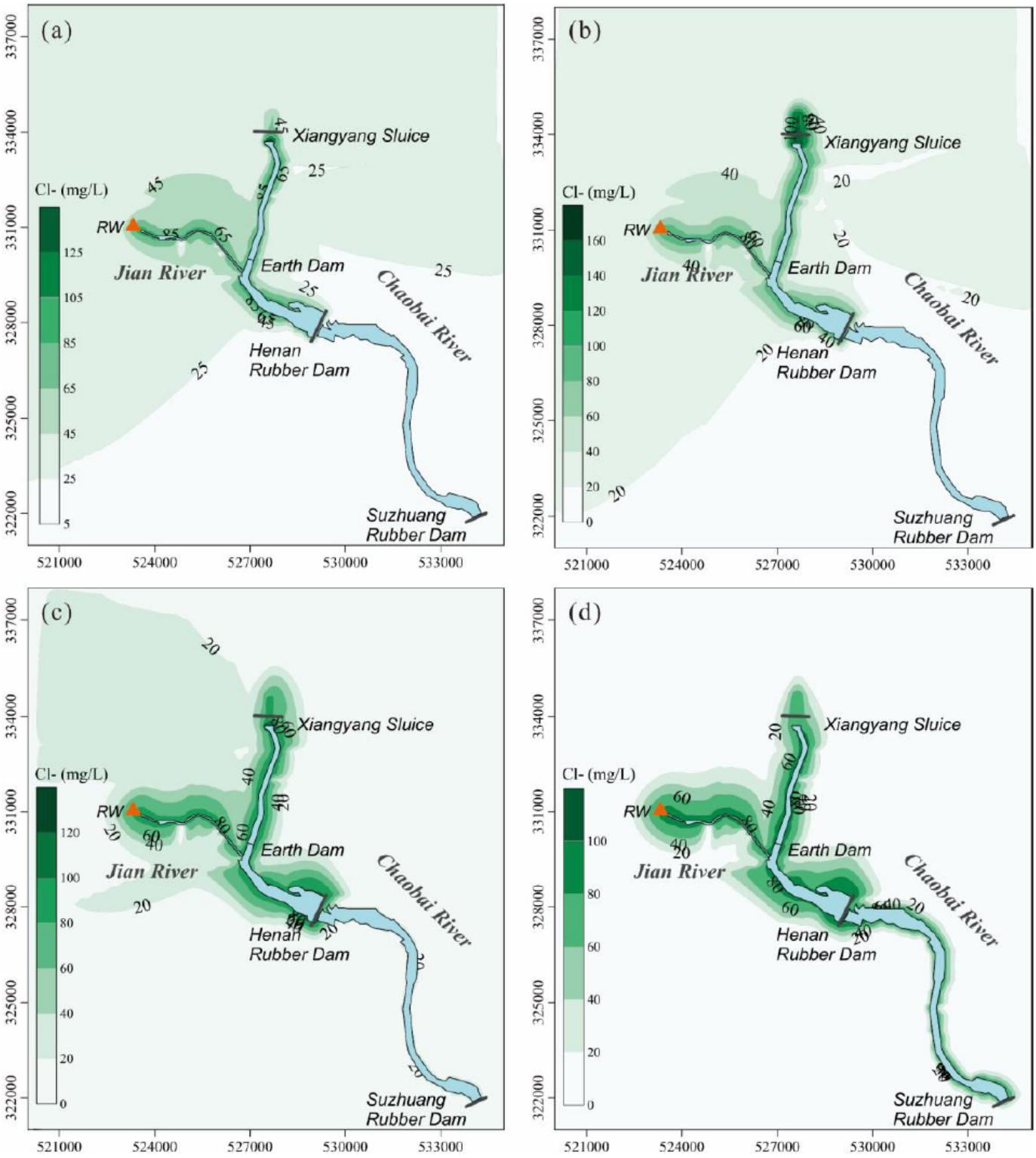

Figure 4

Distribution of the simulated Cl- concentrations in the unconfined aquifer at the end of 2008 (a), 2009 (b), 2012 (c), and 2017 (d) after RW restoring the river channel

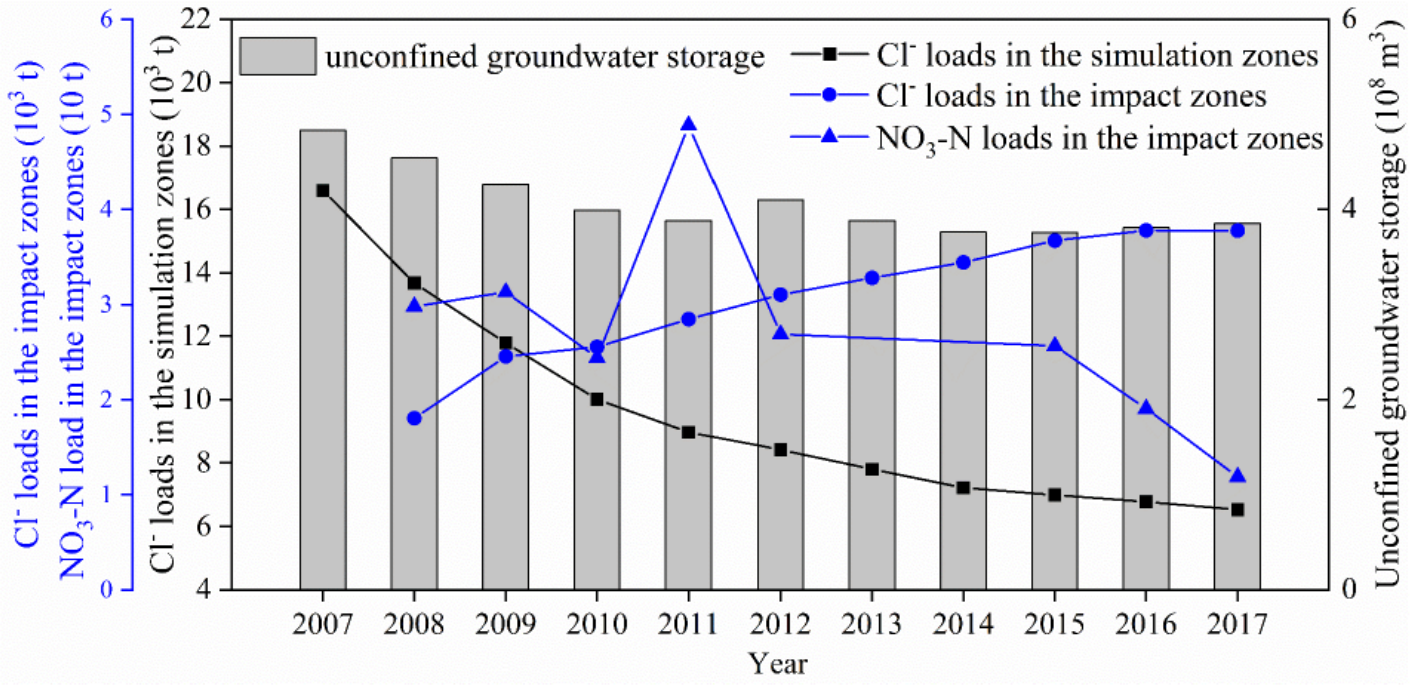

Figure 5

Variations of the unconfined groundwater storage, Cl- loads in the model area, Cl- loads, and NO3-N loads in the affected zones

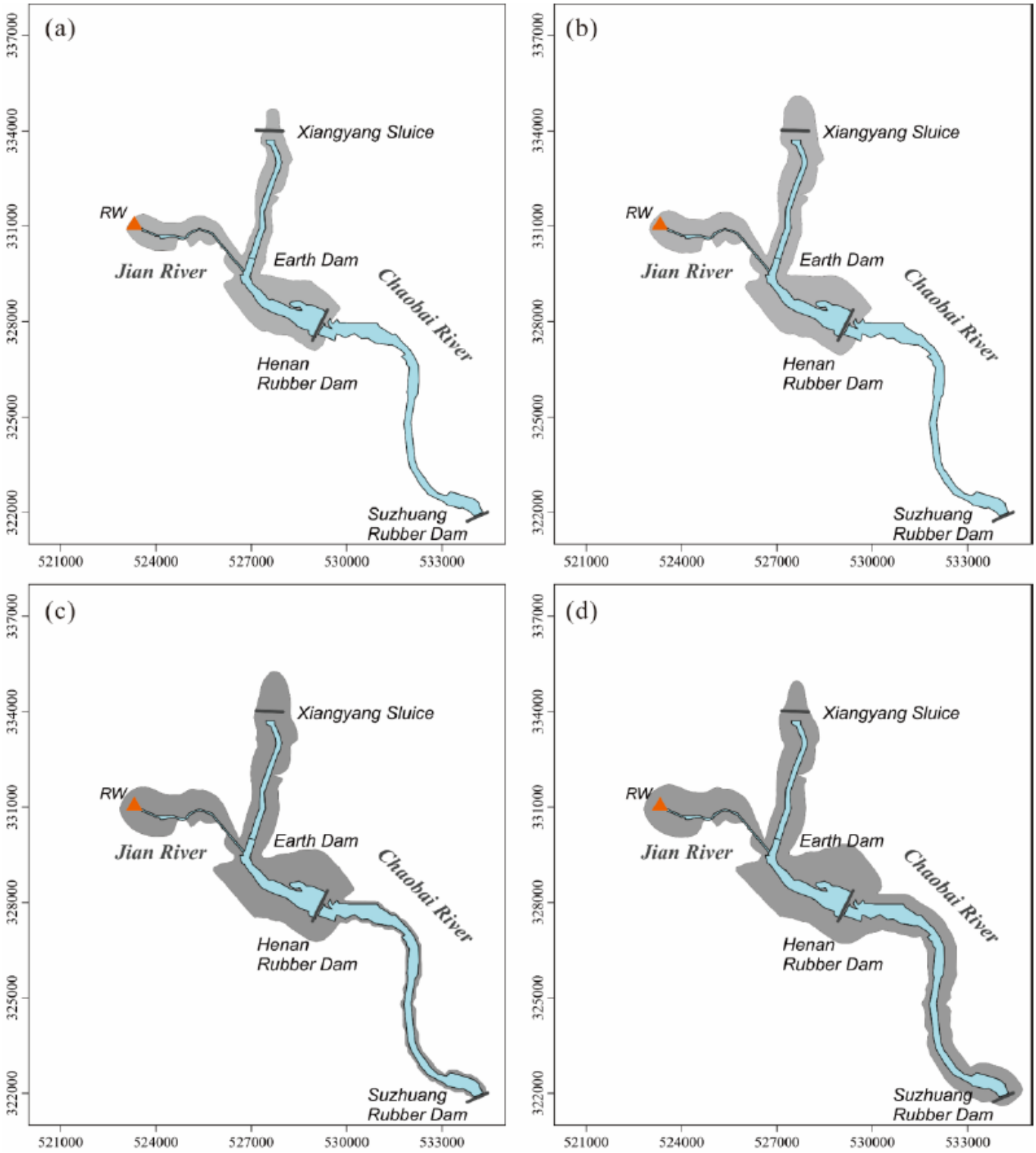

Figure 6

The zones affected by RW for the unconfined aquifer (grey area) at the end of 2008 (a), 2009 (b), 2012 (c), and 2017 (d) after RW restoring the river channel

Supplementary Files

This is a list of supplementary files associated with this preprint. Click to download.

- SupplementaryMaterials.docx